Physica A 466 (2017) 1–9

Contents lists available at ScienceDirect

Physica A

journal homepage: www.elsevier.com/locate/physa

Analysis of the traffic running cost in a two-route system with feedback strategy

Tie-Qiao Tang [a], Qiang Yu [a], Kai Liu [b,*]

[a] School of Transportation Science and Engineering, Beijing Key Laboratory for Cooperative Vehicle Infrastructure Systems and Safety Control, Beihang University, Beijing 100191, China

[b] School of Transportation and Logistics, Dalian University of Technology, Dalian 116024, China

HIGHLIGHTS

- We defined MVFS and NVFS based on the car-following model in a two-route system.
- We explored the effects of MVFS on each vehicle's running cost and each route's total cost.
- We explored the impacts of NVFS on each vehicle's running cost and each route's total cost.

ARTICLE INFO

Article history:
Received 3 June 2016
Received in revised form 11 August 2016
Available online 29 August 2016

Keywords:
Car-following model
Network
Feedback strategy

ABSTRACT

In this paper, we apply the FVD (full velocity difference) model to study the influences of MVFS (mean velocity feedback strategy) and NVFS (the number of vehicles feedback strategy) on each vehicle's running cost and each route's total cost in a two-route system from the numerical perspective. The numerical results illustrate that MFVS and NVFS have significant effects on each vehicle's running cost and each route's total cost, and that the impacts, each vehicle's running cost and each route's total cost are related to the gap of each vehicle's departure time at the origin.

1. Introduction

To date, traffic congestion has been a challenged topic in many fields (e.g., transportation, internet, communication, etc.). In real traffic system, traffic congestion produces some related traffic issues (e.g., safety, energy, emissions, etc.) and the traffic problems have been a big issue all over the word and attracted researchers to propose many traffic flow models or to develop many related technologies (e.g., intelligent transportation system, ITS) [1–4]. The information guidance strategies have been looked on as a better way of relieving congestion and reducing energy consumption and emissions with the rapid development of ITS, so some feedback strategies (FSs) have been proposed to explore the traffic phenomena in a two-route network [5–19]. In the above FSs, researchers assumed that the feedback information is completely accurate and that drivers can definitely choose their best-condition route [20]. In fact, the traffic information is not very accurate. In order to accurately describe the traffic information, Zhao et al. introduced the bounded rationality into the FSs to study the approaching system equilibrium with accurate or not accurate feedback information in a two-route system [21,22].

* Corresponding author.
E-mail address: liukai@dlut.edu.cn (K. Liu).

http://dx.doi.org/10.1016/j.physa.2016.08.066

CA (cellular automaton) model has been used to study each vehicle's motion in the FSs, but car-following model is not introduced into the FSs. Car-following model can reproduce many complex traffic phenomena, so we in this paper use it to study each vehicle's running cost under different FSs in a two-route system. In comparison with the existing studies, this paper has a contribution, i.e., car-following model is used to explore each vehicle's motion under different FSs in a two-route system and the effects of FSs on each vehicle's running cost. This paper is organized as follows: the related models and the related running costs are introduced in Section 2; some numerical tests are conducted to explore the effects of FSs on the related running costs in a two-route system in Section 3; and conclusions are summarized in Section 4.

2. Model formulation

The car-following model on a single-lane road can be formulated as follows:

$$\frac{\mathrm{d}v_n}{\mathrm{d}t} = f\left(v_n, \Delta x_n, \Delta v_n, \ldots\right), \tag{1}$$

where $\frac{\mathrm{d}v_n}{\mathrm{d}t}$, v_n, Δx_n, Δv_n, are the nth vehicle's acceleration, speed, headway, and relative speed, respectively. Eq. (1) just indicates that the nth vehicle's acceleration is determined by its speed, headway, relative speed and other factors. If we define Eq. (1) as different equations, we can obtain different car-following models, e.g., the optimal velocity (OV) model [23] and its extended versions [24,25], the generalized force (GF) model [26] and the full velocity difference (FVD) model [27]. The model [27] is very simple and can reproduce many complex traffic phenomena, so we in this paper use it to describe each vehicle's motion in a two-route system, where the FVD model [27] can be formulated as follows:

$$\frac{\mathrm{d}v_n}{\mathrm{d}t} = \kappa\left(V\left(\Delta x_n\right) - v_n\right) + \lambda \Delta v_n, \tag{2}$$

where κ, λ are two reaction coefficients and $V\left(\Delta x_n\right)$ is the nth vehicle's optimal speed. Jiang et al. [27] defined κ, λ, $V\left(\Delta x_n\right)$ as follows:

$$\kappa = 0.41, \qquad \lambda = \begin{cases} 0.5, & \text{if } \Delta x_n \le 100 \\ 0, & \text{otherwise}, \end{cases} \tag{3}$$

$$V\left(\Delta x_n\right) = V_1 + V_2 \tanh\left(C_1\left(\Delta x_n - l_c\right) - C_2\right), \tag{4}$$

where l_c is the vehicle's average length; V_1, V_2, C_1, C_2 are four parameters. Here, the parameters V_1, V_2, C_1, C_2, l_c are defined as follows [27]:

$$V_1 = 6.75 \text{ m/s}, \qquad V_2 = 7.91 \text{ m/s}, \qquad C_1 = 0.13 \text{ m}^{-1}, \qquad C_2 = 1.57, \qquad l_c = 5 \text{ m}. \tag{5}$$

Note: we can obtain similar results if in this paper, we use other car-following models to describe each vehicle's motion. In this paper we explore each vehicle's running cost in a two-route system, so we should here define the running costs. For simplicity, we here assume that each driver and each vehicle are both homogeneous, so we can define each driver's three running costs in a two-route system as follows:

$$T_n^{\mathrm{I}} = \alpha t_n, \tag{6a}$$

$$T_n^{\mathrm{II}} = \alpha t_n + \beta\,(\mathrm{FC})_n, \tag{6b}$$

$$T_n^{\mathrm{III}} = \alpha t_n + \beta\,(\mathrm{FC})_n + \gamma_1\,(\mathrm{HC})_n + \gamma_2\,(\mathrm{CO})_n + \gamma_3\,(\mathrm{NO}_X)_n, \tag{6c}$$

where T_n^{I}, T_n^{II}, T_n^{III} are the nth driver's first, second and third running costs, respectively; α is the value of time; t_n is the nth driver's running time; β is the fuel price; $(\mathrm{FC})_n$ is the nth vehicle's fuel consumption; γ_1, γ_2, γ_3 are the tolls of HC, CO and NO_X, respectively; $(\mathrm{HC})_n$, $(\mathrm{CO})_n$, $(\mathrm{NO}_X)_n$ are the nth vehicle's HC, CO and NO_X, respectively. As for the three running costs, we here give the following notes:

(1) The first running cost only considers the cost of the travel time.
(2) The second running cost includes the cost of the travel time and the cost of the fuel consumption because each driver should care the fuel consumption in his running cost except for the cost of his travel time.
(3) Based on the second running cost, the third running cost includes the toll of emissions. Each driver does not care the toll of emissions in his running cost and few governments charge for emissions, but the pollution resulted by the vehicle's emissions has been very serious and attracted the transportation departments and many researchers to care the emissions, so we consider the toll of emissions in each vehicle's third running cost, but we do not further calibrate the parameters γ_1, γ_2, γ_3 since we do not have the related data. Therefore, we should collect some related data (including the experimental and empirical data) to calibrate the three parameters and further study the third running cost.

Table 1
The related coefficients in Eq. (8) [28,30].

	Fuel	CO	HC	NO_X
$K^e_{0,0}$	−0.679439	0.887447	−0.728042	−1.067682
$K^e_{0,1}$	0.135273	0.148841	0.012211	0.254363
$K^e_{0,2}$	0.015946	0.030550	0.023371	0.008866
$K^e_{0,3}$	−0.001189	−0.001348	−0.000093243	−0.000951
$K^e_{1,0}$	0.029665	0.070994	0.024950	0.046423
$K^e_{2,0}$	−0.000276	−0.000786	−0.000205	−0.000173
$K^e_{3,0}$	0.000001487	0.000004616	0.000001949	0.000000569
$K^e_{1,1}$	0.004808	0.003870	0.010145	0.015482
$K^e_{1,2}$	−0.000020535	0.000093228	−0.000103	−0.000131
$K^e_{1,3}$	5.5409285E−8	−0.000000706	0.000000618	0.000000328
$K^e_{2,1}$	0.000083329	−0.000926	−0.000549	0.002876
$K^e_{2,2}$	0.000000937	0.000049181	0.000037592	−0.00005866
$K^e_{2,3}$	−2.479644E−8	−0.000000314	−0.000000213	0.00000024
$K^e_{3,1}$	−0.000061321	0.000046144	−0.000113	−0.000321
$K^e_{3,2}$	0.000000304	−0.000001410	0.000003310	0.000001943
$K^e_{3,3}$	−4.467234E−9	8.1724008E−9	−1.739372E−8	−1.257413E−8

Thus, we can define three total costs as follows:

$$T^{\mathrm{I}}_{\mathrm{total}} = \sum_{n=1}^{N_0} T^{\mathrm{I}}_n, \tag{7a}$$

$$T^{\mathrm{II}}_{\mathrm{total}} = \sum_{n=1}^{N_0} T^{\mathrm{II}}_n, \tag{7b}$$

$$T^{\mathrm{III}}_{\mathrm{total}} = \sum_{n=1}^{N_0} T^{\mathrm{III}}_n, \tag{7c}$$

where $T^{\mathrm{I}}_{\mathrm{total}}, T^{\mathrm{II}}_{\mathrm{total}}, T^{\mathrm{III}}_{\mathrm{total}}$ are three corresponding total costs, respectively; N_0 is the number of drivers.

Since we need calculate the nth vehicle's fuel consumption and total emissions, we should introduce the vehicle's fuel consumption model and emission model. Many models were developed to study the vehicle's fuel consumption and emissions [28–37], but we use the VT-Micro model [28,30] to calculate each vehicle's fuel consumption and emissions since this model is determined by the vehicle's instantaneous acceleration and speed, and can be written as follows [28,30]:

$$\ln(\mathrm{MOEe}) = \sum_{i=0}^{3}\sum_{j=0}^{3}\left(K^e_{i,j} \times v^i \times \left(\frac{\mathrm{d}v}{\mathrm{d}t}\right)^j\right), \tag{8}$$ [1]

where MOEe is the vehicle's instantaneous fuel consumption (CO, HC or NO_X); $K^e_{i,j}$ is the corresponding regression coefficient (see Table 1).

3. Numerical tests

In this section, we apply the FVD model [27] to study each vehicle's three running costs and the corresponding three total costs in a two-route system under different route-choice rules from the numerical perspective. Since it is difficult to obtain the analytical solution of the FVD model, we should utilize numerical scheme to discretize this model. Many numerical schemes can be used to discretize Eq. (2), but the numerical schemes have no qualitative effects on the numerical results, so we here apply the Euler forward difference to discretize Eq. (2), i.e.,

$$\begin{aligned} v_n(t+\Delta t) &= v_n(t) + \frac{\mathrm{d}v_n(t)}{\mathrm{d}t}\cdot\Delta t \\ x_n(t+\Delta t) &= x_n(t) + v_n(t)\cdot\Delta t + \frac{1}{2}\frac{\mathrm{d}v_n(t)}{\mathrm{d}t}\cdot(\Delta t)^2, \end{aligned} \tag{9}$$

where $\Delta t = 0.1$ s is the time-step length.

[1] Note: if using other models to calculate each vehicle's fuel consumption and emissions, we can obtain similar results; but we do not explore the effects of different models on each vehicle's fuel consumption and emissions since this topic is beyond of the scope of this paper.

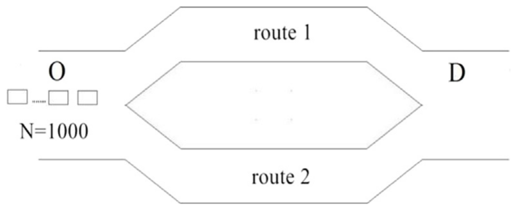

Fig. 1. The scheme of a two-route system.

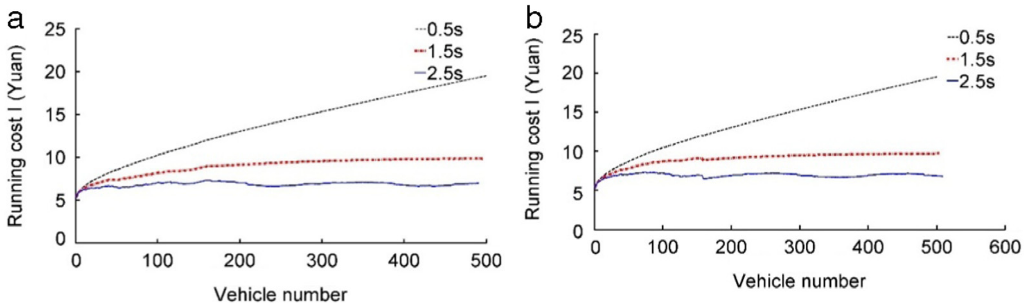

Fig. 2. Each vehicle's first running cost under MVFS, where (a) is route 1 and (b) is route 2.

Before exploring each vehicle's running costs in a two-route system (see Fig. 1), we should first make the following assumptions:

(a) L_i $(i = 1, 2) = 10\,000$ m is the length of route i.
(b) $\Delta t_{n,0} = t_{n,0} - t_{n-1,0}$ $(n > 1)$ is a constant, where $t_{n,0}$ is the departure time of the nth vehicle at the origin.
(c) Any driver will automatically leave the network when he gets to D, i.e., his following vehicle will be the leading one on his route.
(d) $N = 1000$ is the number of drivers in the two-route system.
(e) We study the impacts of MVFS (mean velocity FS) and NVFS (the number of vehicles FS) on each vehicle's three running costs and the corresponding total costs in the two-route system (see Fig. 1). The MVFS is defined as follows: when $\frac{1}{M_1}\sum_{j=1}^{M_1} v_{j,1} \geq \frac{1}{M_2}\sum_{j=1}^{M_2} v_{j,2}$, the kth vehicle chooses route 1; otherwise, the kth vehicle chooses route 2. The NVFS is defined as follows: when $M_1 \leq M_2$, the kth vehicle chooses route 1; otherwise, the kth vehicle at O chooses route 2. Note: $v_{j,i}$ is the jth vehicle's velocity on route 1 and M_i is the number of vehicles on route i.

Other parameters are defined as follows:

$$\alpha = 0.01\ \text{RMB/s}, \qquad \beta = 7.81\ \text{RMB/L}, \qquad \gamma_1 = \gamma_2 = 0.5\ \text{RMB/g}, \qquad \gamma_3 = 1\ \text{RMB/g}. \tag{10}$$

3.1. Each vehicle's running cost and the corresponding total cost under MVFS

First, we study each vehicle's first running cost and each route's first total cost under MVFS (see Figs. 2 and 3). From Figs. 2 and 3, we have:

(1) each vehicle's first running cost increases with its series number on each route, but no prominent difference exists between the two routes. Qualitatively speaking, the phenomena are completely consistent with the numerical results in Ref. [38], which indicates that MVFS does not change the properties of each vehicle's running cost.
(2) with the increase of $\Delta t_{n,0}$ $(n > 1)$, each vehicle's first running cost drops, but the differences increase with its series number.
(3) when $\Delta t_{n,0}$ $(n > 1)$ increases, each route's total running cost first prominently drops and then gradually becomes to a constant.
(4) no prominent differences (including each vehicle's running cost and the total running cost) exist between the two routes since the lengths of the two routes are equal.

Next, we study each vehicle's second running cost and each route's second total cost under MVFS (see Figs. 4 and 5). From Figs. 4 and 5, we have:

(1) Compared to Figs. 2 and 3, MVFS has no prominent influence on the second running cost, i.e., Fig. 4 is qualitatively similar to Fig. 2 and Fig. 5 is qualitatively similar to Fig. 3.
(2) Each vehicle's second running cost is larger than its first running cost and each route's second total cost is larger than its first total cost, but the differences are related to $\Delta t_{n,0}$ $(n > 1)$, i.e., the differences first sharply drop and then eventually turn a constant when $\Delta t_{n,0}$ $(n > 1)$ increases since each vehicle's fuel consumption first drops and then become stable.

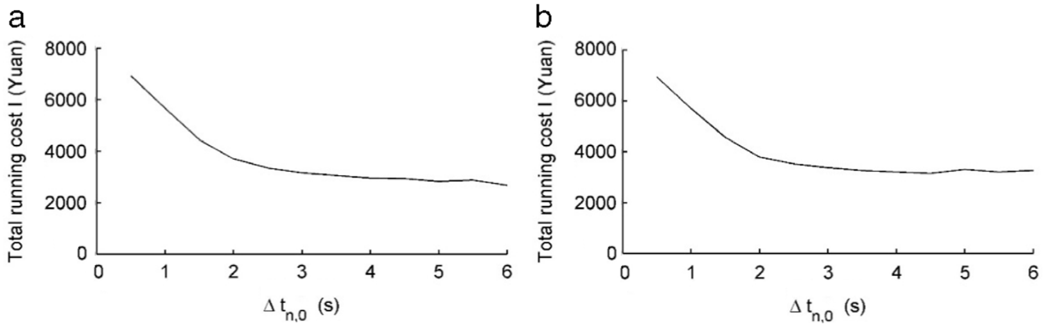

Fig. 3. Each route's first total cost under MVFS, where (a) is route 1 and (b) is route 2.

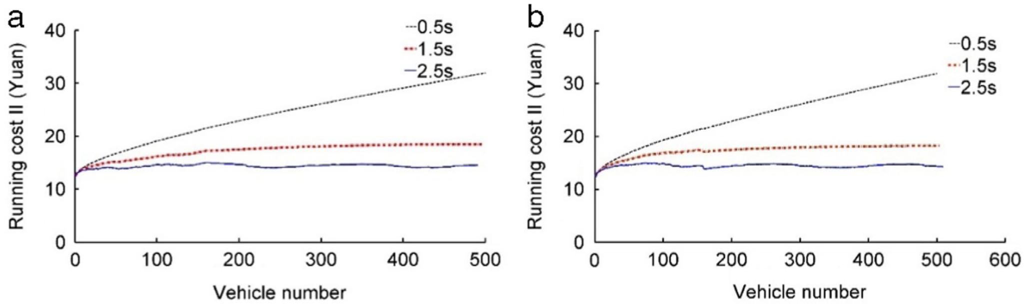

Fig. 4. Each vehicle's second running cost under MVFS, where (a) is route 1 and (b) is route 2.

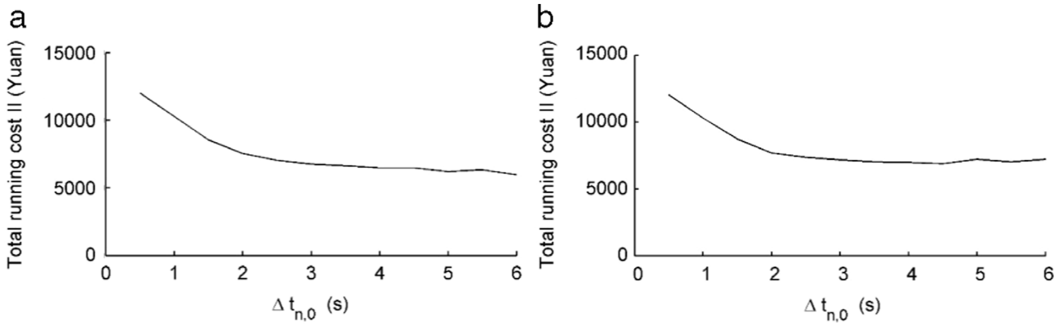

Fig. 5. Each route's second total cost under MVFS, where (a) is route 1 and (b) is route 2.

Finally, we explore each vehicle's third running cost and each route's third total cost under MVFS (see Figs. 6 and 7). From the two figures, we have: compared to Figs. 4 and 5, MVFS has no prominent effect on the third running cost, i.e., Figs. 6 and 7 are qualitatively similar to Figs. 4 and 5, respectively; each vehicle's third running cost is larger than its second running cost and each route's third total cost is larger than its second total cost, but the differences are very complex and related to $\Delta t_{n,0}$ $(n > 1)$.[2]

3.2. Each vehicle's running cost and each route's total cost under NVFS

In this subsection, we explore the effects of NVFS on each vehicle's first, second and third running costs, and each route's corresponding total costs (see Figs. 8–13). We have:

(1) Figs. 8 and 9 are respectively similar to Figs. 2 and 3. This shows that the influence of NVFS on each vehicle's first running cost and each route's first total cost are qualitatively the same as those of MVFS.
(2) some vehicles' first running costs are slightly reduced (especially when the traffic is relatively congested), so the first total running cost is slightly reduced (especially when the traffic is relatively congested). This indicates that the effect of NVFS on the traffic system is slightly better than those of MVFS (especially when the traffic is relatively congested).

[2] Note: we do not further explore this topic in this paper since the fuel consumption and emissions are very complex and beyond the topic of this paper.

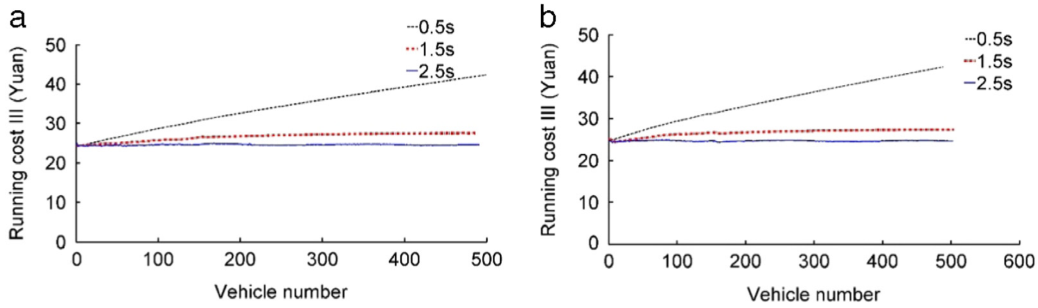

Fig. 6. Each driver's third running cost under MVFS, where (a) is route 1 and (b) is route 2.

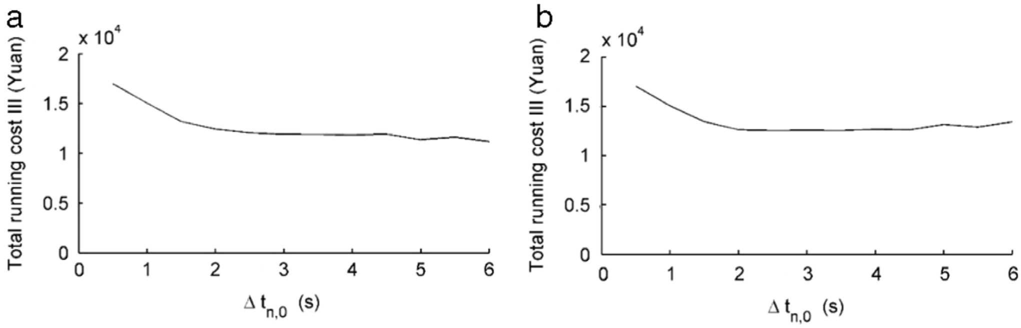

Fig. 7. Each route's third total cost under MVFS, where (a) is route 1 and (b) is route 2.

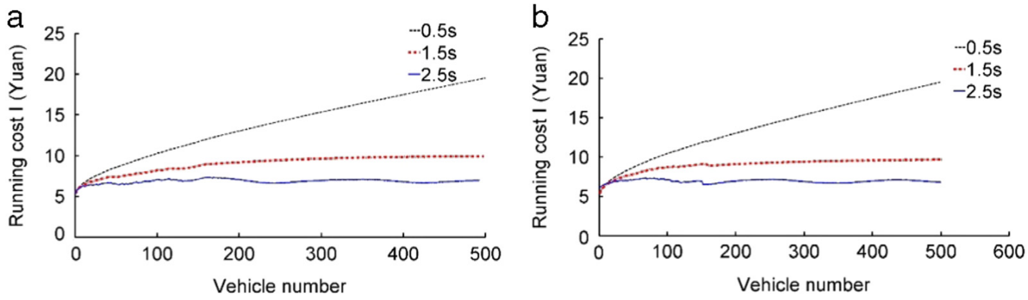

Fig. 8. Each vehicle's first running cost under NVFS, where (a) is route 1 and (b) is route 2.

From Figs. 10 and 11, we have:

(1) Considering the fuel consumption does not change the impacts of NVFS on each vehicle's running cost, i.e., Figs. 10 and 11 are respectively similar to Figs. 8 and 9.

(2) NVFS can slightly reduce some vehicles' second running costs on each route and each route's second total cost (especially when the traffic is relatively congested), so these vehicles' second running costs on each route and each route's second cost are slightly lower than the ones under MVFS (especially when the traffic is relatively congested). This shows that the influence of NVFS on the traffic system is slightly better than those of MVFS (especially when the traffic is relatively congested).

From Figs. 12 and 13, we have:

(I) the toll of emissions does not change the influence of NVFS on each vehicle's running cost, i.e., Figs. 12 and 13 are respectively similar to Figs. 8 and 9.

(II) NVFS can slightly reduce some vehicles' third running costs on each route and each route's third total cost (especially when the traffic is relatively congested), so the vehicles' third running costs on each route and each route's third cost are slightly lower than the ones under MVFS (especially when the traffic is relatively congested). This shows that the influence of NVFS on the traffic system is slightly better than those of MVFS (especially when the traffic is relatively congested).

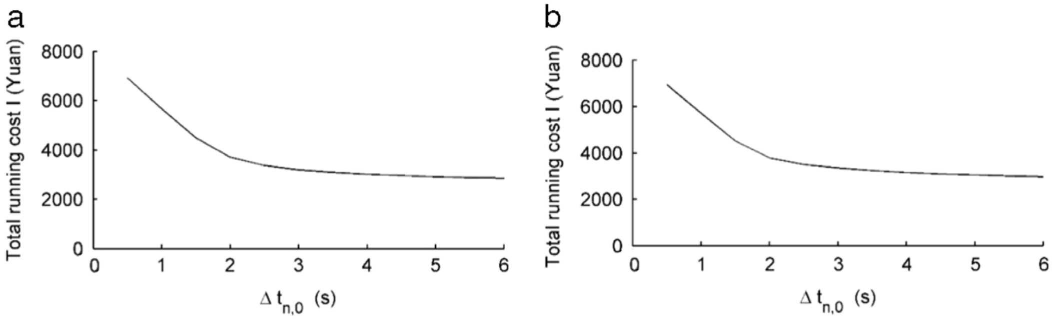

Fig. 9. Each route's first total cost and $\Delta t_{n,0}$ ($n > 1$) under NVFS, where (a) is route 1 and (b) is route 2.

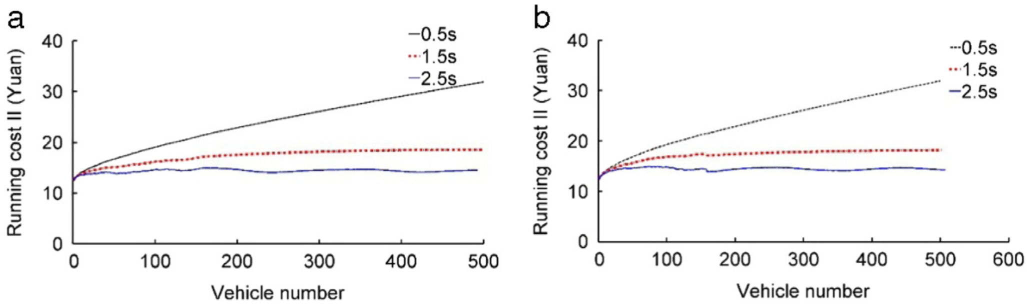

Fig. 10. Each vehicle's second running cost under NVFS, where (a) is route 1 and (b) is route 2.

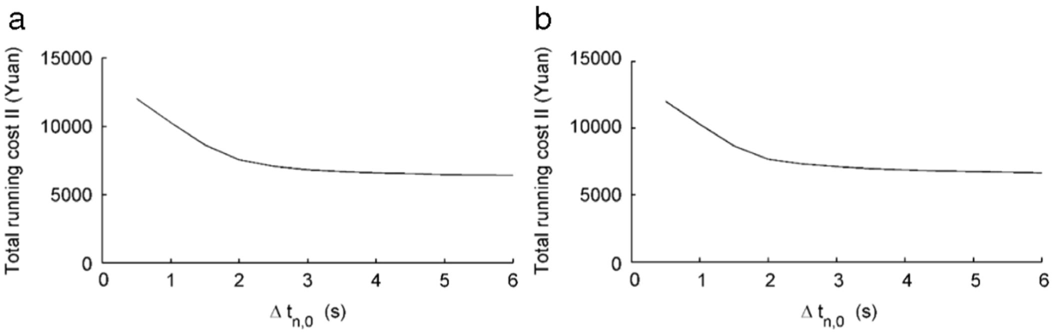

Fig. 11. Each route's second total cost under NVFS, where (a) is route 1 and (b) is route 2.

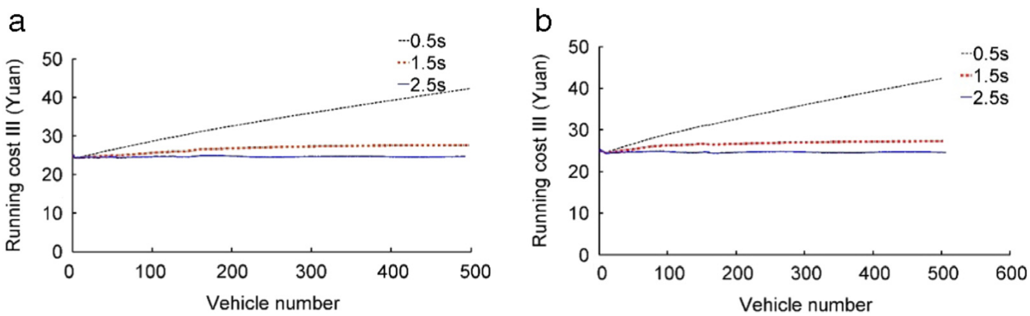

Fig. 12. Each driver's third running cost under NVFS, where (a) is route 1 and (b) is route 2.

4. Conclusion

Many traffic flow models are developed to study the complex traffic phenomena in a two-route system, but little effort has been made to study the effects of FS on each vehicle's running cost and each route's total cost from the perspective of the car-following model. In this paper, we use the car-following model [27] to explore each vehicle's running cost and

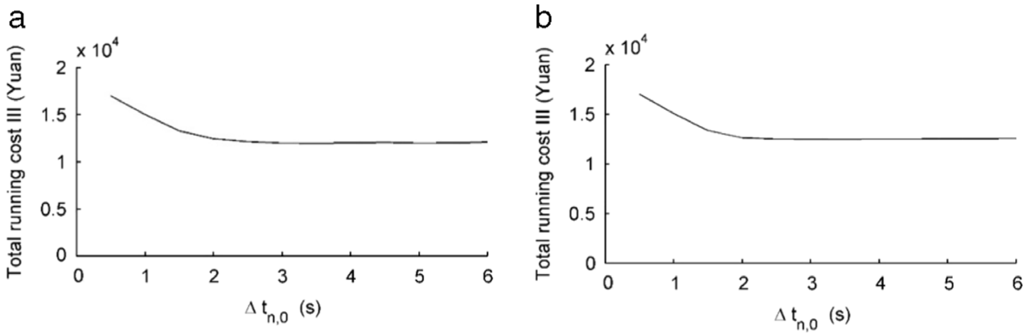

Fig. 13. Each route's third total cost under NVFS, where (a) is route 1 and (b) is route 2.

each route's total cost in a two-route system under MVFS and NVFS from the numerical perspective. The numerical results indicate that each vehicle's running cost and each route's total cost are both dependent on the gap of the departure time and that NVFS is a little better than MVFS (especially when the traffic is relatively congested). However, this study still has the following limitations:

(a) We only investigate the impacts of MVFS and NVFS on each vehicle's three running costs and the corresponding total costs.
(b) We do not use the empirical/experimental data to calibrate the models, parameters and numerical results.
(c) We do not use macro traffic flow model to explore the impacts of NVFS and MVFS on the three running costs in a two-route system.

In view of the above limitations, we will use empirical/experimental data to propose more exact car-following model, fuel consumption model and emission model to study each vehicle's running cost and the system's total cost under other route choice behavior. In addition, we will apply the macro traffic flow models [39–44] to explore each vehicle's running cost and the system's total cost under different route choice behaviors.

Acknowledgment

This work has been supported by the National Natural Science Foundation of China (71422001; 71271016).

References

[1] D. Chowdhury, L. Santen, A. Schadschneider, Statistical Physics of vehicular traffic and some related systems, Phys. Rep. 329 (2000) 199–329.
[2] D. Helbing, Traffic and related self-driven many-particle system, Rev. Modern Phys. 73 (2001) 1067–1141.
[3] J.N. Barkenbus, Eco-driving: An overlooked climate change initiative, Energy Policy 38 (2010) 762–769.
[4] E. Gilman, A. Keskinarkaus, S. Tamminen, S. Pirttikangas, J. Roning, J. Riekki, Personalised assistance for fuel-efficient driving, Transp. Res. C 71 (2015) 681–705.
[5] J. Whale, A. Bazzan, F. Klugl, M. Schreckenberg, Decision dynamics in a traffic scenario, Physica A 287 (2000) 669–681.
[6] J. Whale, A. Bazzan, F. Klugl, M. Schreckenberg, The impact of real-time information in a two-route scenario, Transp. Res. C 10 (2002) 399–417.
[7] K. Lee, P. Hui, B. Wang, N. Johnson, Effects of announcing global information in a two-route traffic model, J. Phys. Soc. Japan 70 (2001) 3507–3510.
[8] W. Wang, B. Wang, W. Zheng, C. Yin, T. Zhou, Advanced information feedback in intelligent traffic systems, Phys. Rev. E 72 (2005) 066702.
[9] C. Dong, X. Ma, B. Wang, Weighted congestion coefficient feedback in intelligent transportation systems, Phys. Lett. A 374 (2010) 1326–1331.
[10] C. Dong, X. Ma, B. Wang, Advanced information feedback strategy in intelligent two-route traffic flow systems, Sci. China Inf. Sci. 53 (2010) 2265–2271.
[11] C. Dong, X. Ma, G. Wang, X. Sun, B. Wang, Advanced information feedback strategy in intelligent two-route traffic flow systems, Physica A 388 (2009) 4561–4567.
[12] C. Dong, X. Ma, G. Wang, B. Wang, X. Sun, Projected dynamical systems in the formulation, stability analysis, and computation of fixed-demand traffic network equilibria, Physica A 389 (2010) 3274–3281.
[13] B. Chen, W. Tong, W. Zhang, X. Sun, B. Wang, Flux information feedback strategy in intelligent traffic systems, Europhys. Lett. 97 (2012) 14001.
[14] B. Chen, W. Tong, W. Zhang, X. Sun, B. Wang, Real-time information feedback based on a sharp decay weighted function, Comput. Phys. Comm. 183 (2012) 2081–2088.
[15] B. Chen, Y. Xie, W. Tong, C. Dong, D. Shi, B. Wang, A comprehensive study of advanced information feedbacks in real-time intelligent traffic systems, Physica A 391 (2012) 2730–2739.
[16] K. Tobita, T. Nagatani, Effect of signals on two-route traffic system with real-time information, Physica A 391 (2012) 6137–6145.
[17] K. Tobita, T. Nagatani, Green-wave control of unbalanced two-route traffic system with signals, Physica A 392 (2013) 5422–5430.
[18] Y. Hino, T. Nagatani, Effect of bottleneck on route choice in two-route traffic system with real-time information, Physica A 395 (2014) 425–433.
[19] Y. Hino, T. Nagatani, Asymmetric effect of route-length difference and bottleneck on route choice in two-route traffic system, Physica A 428 (2015) 416–425.
[20] X. Guo, H. Liu, Bounded rationality and irreversible network change, Phys. Lett. A 45 (2011) 1606–1618.
[21] X.M. Zhao, D.F. Xie, Z.Y. Gao, L. Gao, Equilibrium of a two-route system with delayed information feedback strategies, Phys. Lett. A 377 (2013) 3161–3169.
[22] X.M. Zhao, D.F. Xie, Q. Li, Approaching system equilibrium with accurate or not accurate feedback information in a two-route system, Comput. Phys. Comm. 187 (2015) 106–114.
[23] M. Bando, K. Hasebe, A. Nakayama, A. Shibata, Y. Sugiyama, Dynamical model of traffic congestion and numerical simulation, Phys. Rev. E 51 (1995) 1035–1042.
[24] T. Nagatani, Stabilization and enhancement of traffic flow by next-nearest-neighbor interaction, Phys. Rev. E 60 (1999) 6395–6401.

[25] H.X. Ge, S.Q. Dai, L.Y. Dong, Y. Xue, Stabilization effect of traffic flow in an extended car-following model based on an intelligent transportation system application, Phys. Rev. E 70 (2004) 066134.
[26] D. Helbing, B. Tilch, Generalized force model of traffic dynamics, Phys. Rev. E 58 (1998) 133–138.
[27] R. Jiang, Q.S. Wu, Z.J. Zhu, Full velocity difference model for car-following theory, Phys. Rev. E 64 (2001) 017101.
[28] K. Ahn, Microscopic fuel consumption and emission modeling (Dissertation for Master Degree), Virginia Polytechnic Institute and State University, Blacksburg, 1998.
[29] H. Rakha, M. Van Aerde, K. Ahn, A. Trani, Requirements for evaluating traffic signal control impacts on energy and emissions based on instantaneous speed and acceleration measurements, Transp. Res. Rec. 1738 (2000) 56–67.
[30] K. Ahn, H. Rakha, A. Trani, M. Van Aerde, Estimating vehicle fuel consumption and emissions based on instantaneous speed and acceleration levels, J. Transp. Eng. 128 (2002) 182–190.
[31] H.O. Gao, D.A. Niemeier, The impact of rush hour traffic and mix on the ozone weekend effect in southern California, Transp. Res. D 12 (2007) 83–98.
[32] D.B. Sonntag, H.O. Gao, Developing link-based particle number emission models for diesel transit buses using engine and vehicle parameters, Transp. Res. D 14 (2009) 240–248.
[33] Y. Kamarianakis, H.O. Gao, Accounting for exhaust gas transport dynamics in instantaneous emission models via smooth transition regression, Environ. Sci. Technol. 44 (2010) 1320–1326.
[34] H.O. Gao, R.A. Klein, Environmental equity in funding decisions of the clean air school bus program: the case of New York State, Transp. Res. D 16 (2011) 10–14.
[35] Y. Kamarianakis, H.O. Gao, Evaluating effects of engine operating variables on particle number emission rates using robust regression models, Transp. Res. Rec. 2233 (2011) 36–44.
[36] H.A. Rakha, K. Ahn, K. Moran, B. Saerens, E. Van den Bulck, Virginia Tech comprehensive power-based fuel consumption model: model development and testing, Transp. Res. D 16 (2011) 492–503.
[37] D.B. Sonntag, H.O. Gao, B.A. Holmen, Comparison of particle mass and number emissions from a diesel transit bus across temporal and spatial scales, Transp. Res. D 25 (2013) 146–154.
[38] T.Q. Tang, Q. Yu, H.J. Huang, W.X. Wu, Analyzing the travel time of car-following model on an open road, Modern Phys. Lett. B 29 (2015) 1550055.
[39] A.K. Gupta, P. Redhu, Jamming transition of a two-dimensional traffic dynamics with consideration of optimal current difference, Phys. Lett. A 377 (2013) 2027–2033.
[40] A.K. Gupta, P. Redhu, Analyses of a modified two-lane lattice model by considering the density difference effect, Commun. Nonlinear Sci. Simul. 19 (2014) 1600–1610.
[41] P. Redhu, A.K. Gupta, Phase transition in a two-dimensional triangular flow with consideration of optimal current difference effect, Nonlinear Dynam. 78 (2014) 957–968.
[42] A.K. Gupta, S. Sharma, P. Redhu, Analyses of lattice traffic flow model on a gradient highway, Commun. Theor. Phys. 62 (2014) 393–404.
[43] A.K. Gupta, S. Sharma, P. Redhu, Effect of multi-phase optimal velocity function on jamming transition in a lattice hydrodynamic model with passing, Nonlinear Dynam. 80 (2015) 1091–1108.
[44] P. Redhu, A.K. Gupta, Effect of forward looking sites on a multi-phase lattice hydrodynamic model, Physica A 445 (2016) 150–160.